Cell Reports, Volume *39*

Supplemental information

Longitudinal analyses reveal distinct immune response landscapes in lung and intestinal tissues from SARS-CoV-2-infected rhesus macaques

Huiwen Zheng, Yanli Chen, Jing Li, Heng Li, Xin Zhao, Jiali Li, Fengmei Yang, Yanyan Li, Changkun Liu, Li Qin, Yuanyuan Zuo, Qian Zhang, Zhanlong He, Haijing Shi, Qihan Li, and Longding Liu

Cell Reports, Volume *39*

Supplemental information

Longitudinal analyses reveal distinct immune response landscapes in lung and intestinal tissues from SARS-CoV-2-infected rhesus macaques

Huiwen Zheng, Yanli Chen, Jing Li, Heng Li, Xin Zhao, Jiali Li, Fengmei Yang, Yanyan Li, Changkun Liu, Li Qin, Yuanyuan Zuo, Qian Zhang, Zhanlong He, Haijing Shi, Qihan Li, and Longding Liu

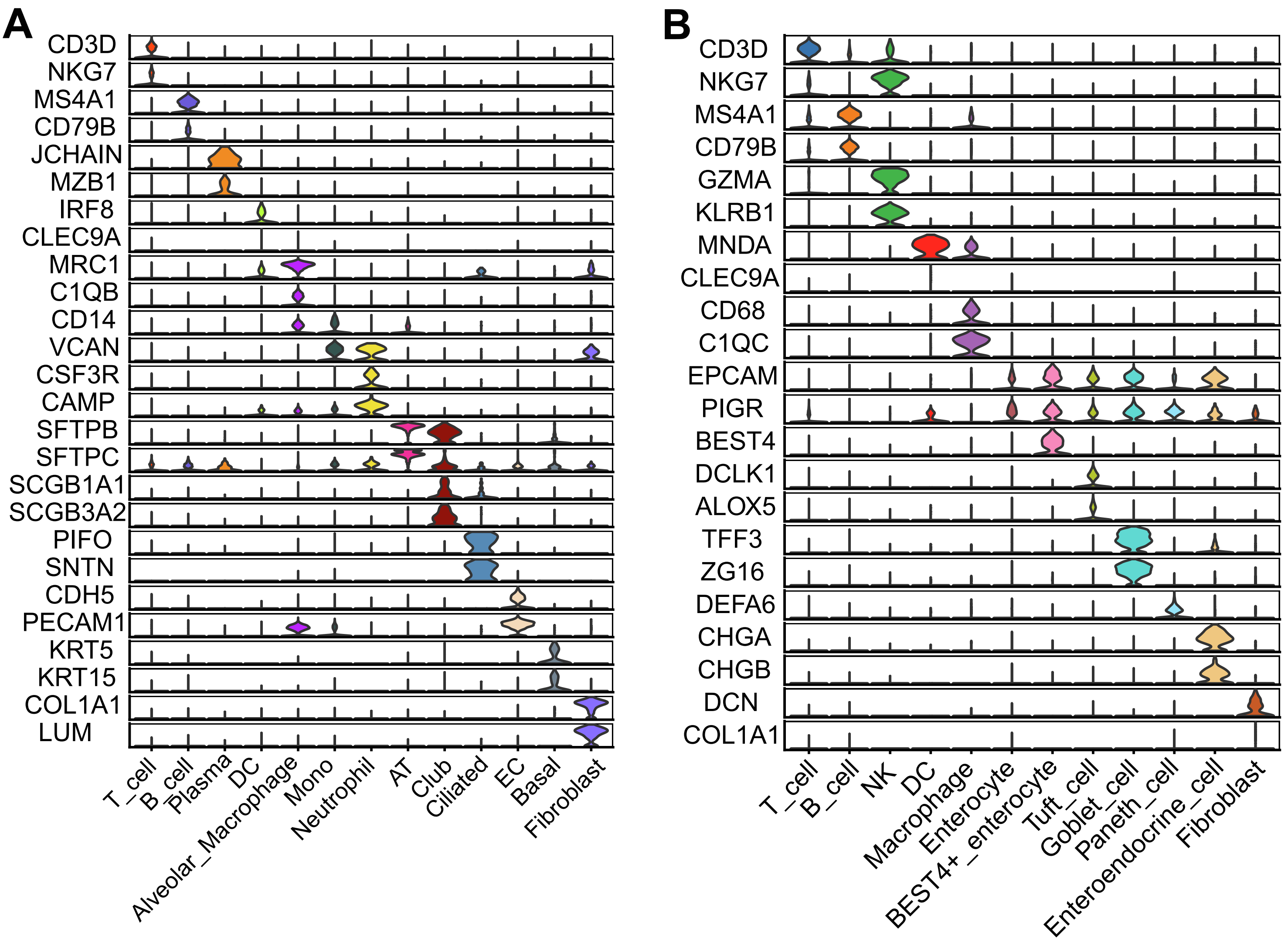

Figure S1: Violin plots showing the expression of characteristic marker genes across cell clusters, related to Figure 2. (A) lung; (B) intestine; the x-axis represents the cell type, and the y-axis represents the normalized gene expression level.

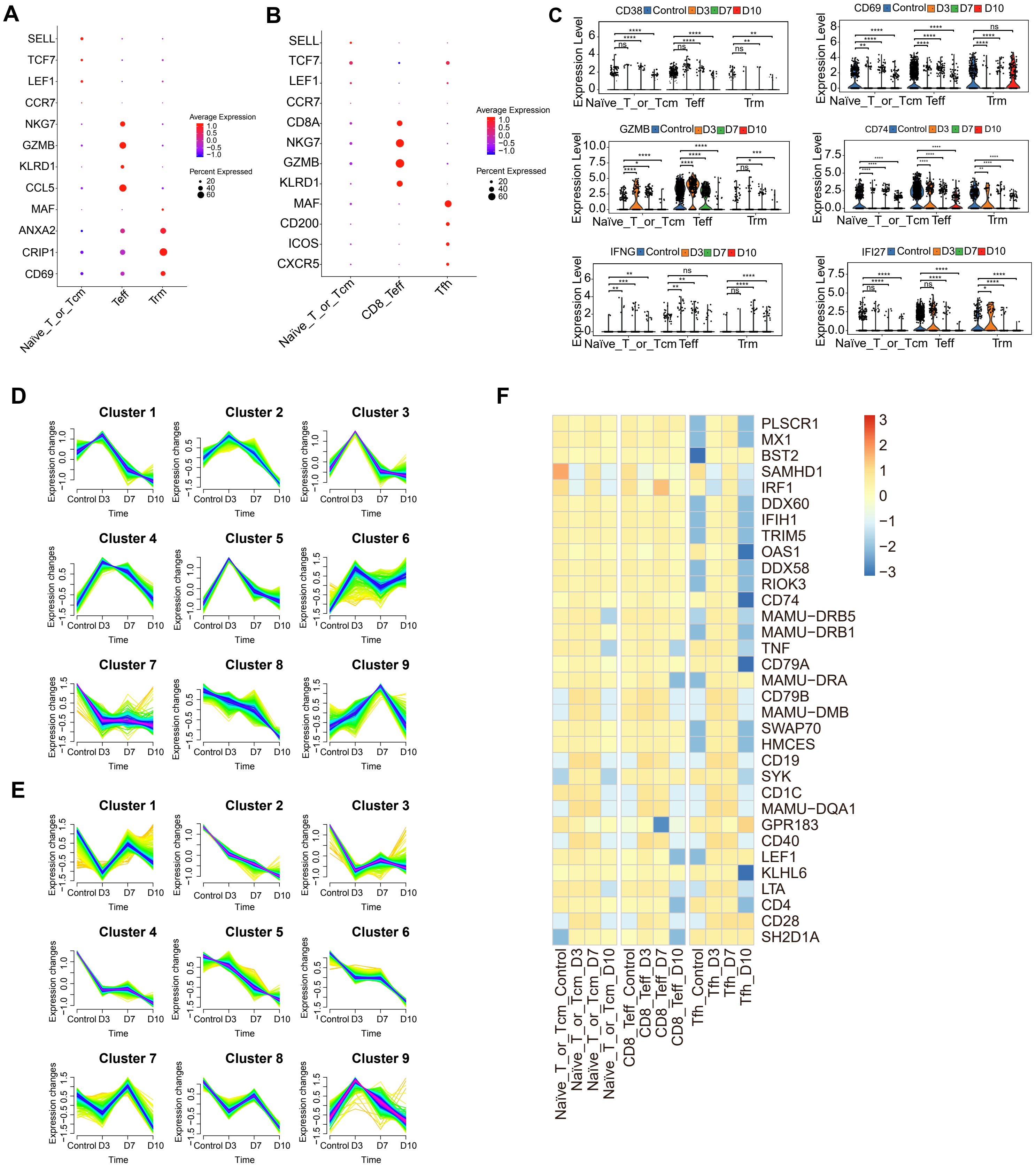

Figure S2: The scRNA-seq dataset for SARS-CoV-2 infected T cell clusters, related to Figure 3. (A) Violin plots showing marker genes of T-cell clusters in the lung. The y-axis represents the normalized gene expression value. (B) Violin plots showing marker genes of T-cell clusters in the intestine. The y-axis represents the normalized gene expression value. (C) The differential expression levels of the T-cell activation-related genes CD38, CD69, GZMB, and CD74 and the interferon stimulation-related genes IFI27 and IFNG in infected samples at 3, 7, 10 dpi and normal control samples in the lung. *p<0.05, **p<0.01, ***p<0.001, ****p<0.0001, Wilcoxon text.(D) Time series analysis of genes of T cells clustered by expression pattern during the progression of SARS-CoV-2 infection in the lung with the mfuzz R package. (E) Time series analysis of genes of T cells clustered by expression pattern during the progression of SARS-CoV-2 infection in the small intestine with the mfuzz R package. (F) Heatmap of genes related with antiviral immune response at different times post-infection (3 dpi, 7 dpi and 10 dpi) in T cell subsets of intestine.

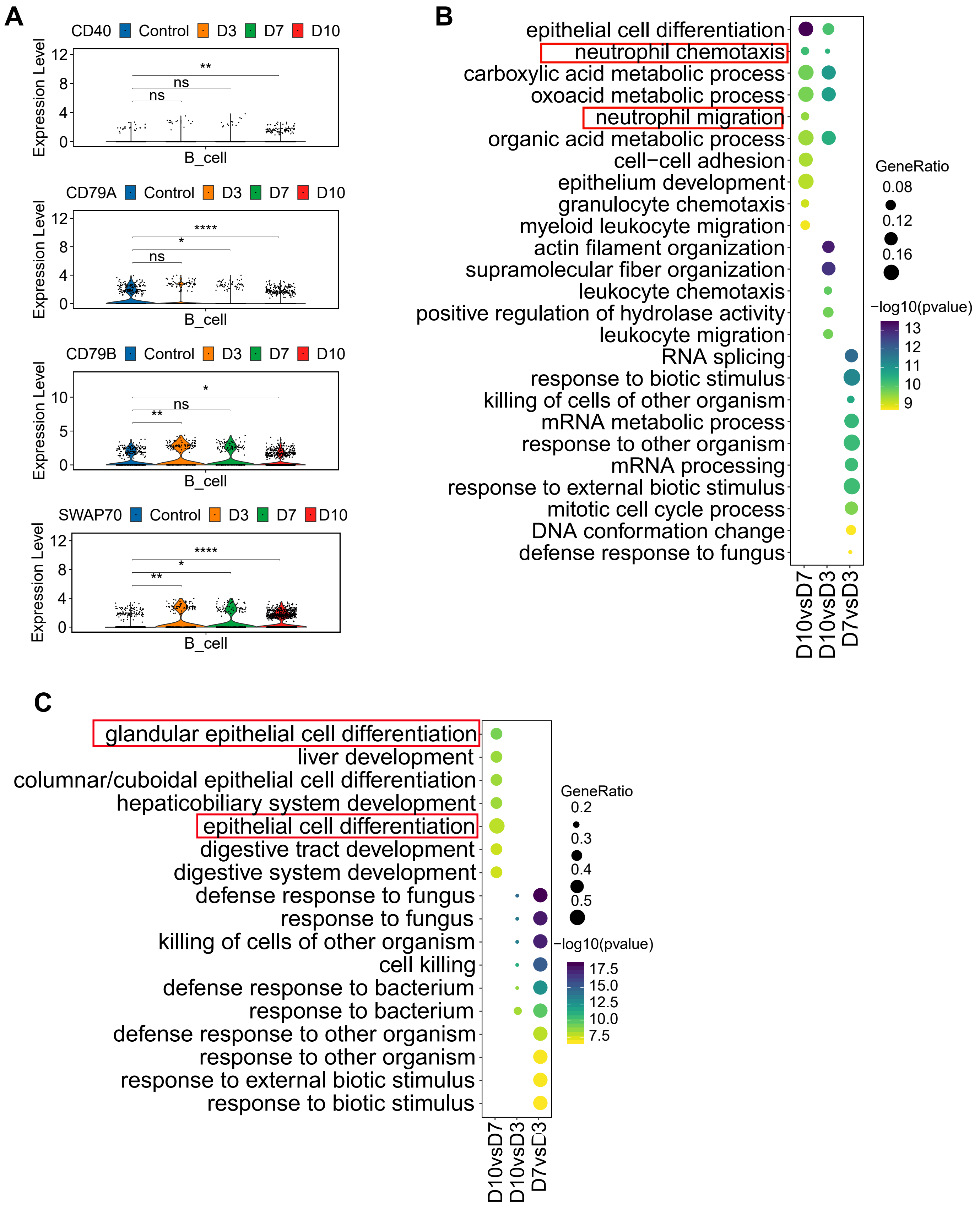

Figure S3: The gene characteristics of infected-associated change in B and Paneth cells related to Figure 4. (A) Violin plots showing activation-related marker genes of B-cell clusters in the lung. The y-axis represents the normalized gene expression value. Statistical analysis to compare the control with different infection timepoints (3 dpi, 7 dpi, and 10 dpi).$*p<0.05$, $**p<0.01$, $****p<0.0001$, Wilcoxon test. (B-C) The top 10 up-enriched GO terms were revealed in SARS-CoV-2-infected macaques at 10 dpi vs. 3 dpi, 10 dpi vs. 7 dpi, and 7 dpi vs. 3 dpi across B-cell clusters(B) and Paneth cells(C) from the intestine.

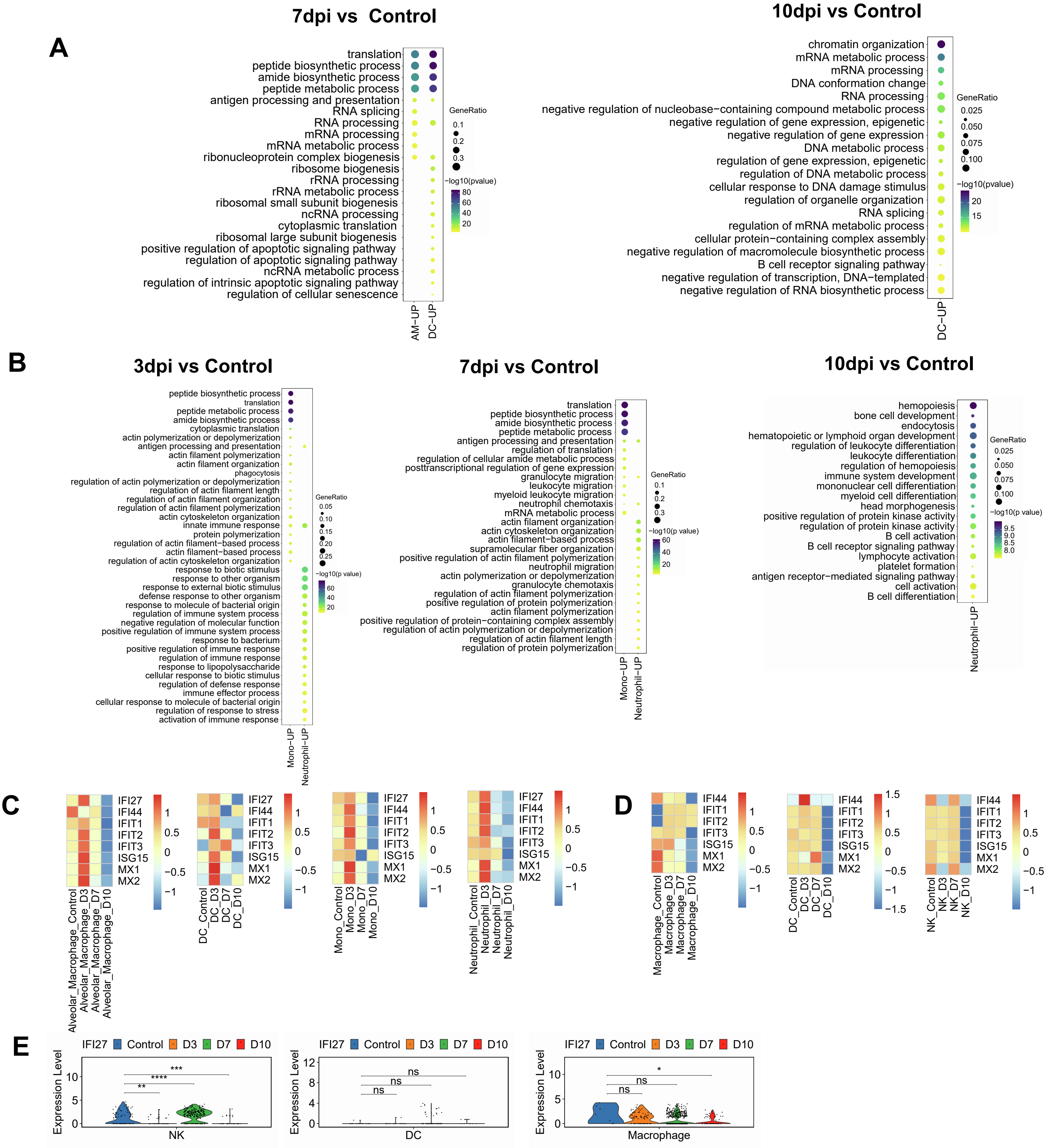

Figure S4: The gene characteristics of infected-associated change in myeloid cell population, related to Figure 5. (A) The top 10 enriched GO terms were revealed in SARS-CoV-2-infected macaques at 7 dpi compared with control across AM, and DC cell clusters from the lung. AMs does not exhibit a significantly enriched term of biological process 10 dpi compared with control, so it is not shown. (B) The top 10 enriched GO terms were revealed in SARS-CoV-2-infected macaques at 3dpi vs.control, 7 dpi vs. control and 10 dpi vs. control across monocytes and neutrophils clusters from the lung. Monocytes do not exhibit a significantly enriched term of biological process 10 dpi cmpared with control , so it is not shown. (C) The differential expression levels of the IFI27, IFI44, IFIT1, IFIT2, IFIT3, ISG15, MX1, and MX2 genes in neutrophils, monocytes, DCs and AMs in infected samples (at 3, 7, and 10 dpi) and the control samples in the lung. (D) The differential expression levels of the IFI44, IFIT1, IFIT2, IFIT3, ISG15, MX1, and MX2 in macrophages, DC and NK cells in infected samples (at 3, 7, and 10 dpi) and the control samples in the small intestine. (E) The differential expression levels of the IFI27 gene in DCs, macrophages and NK cells in infeceted samples (at 3, 7, and 10 dpi) and the control samples in the small intestine.$^*p<0.05$, $^{**}p<0.01$, $^{***}p<0.001$, $^{****}p<0.0001$, Wilcoxon text.

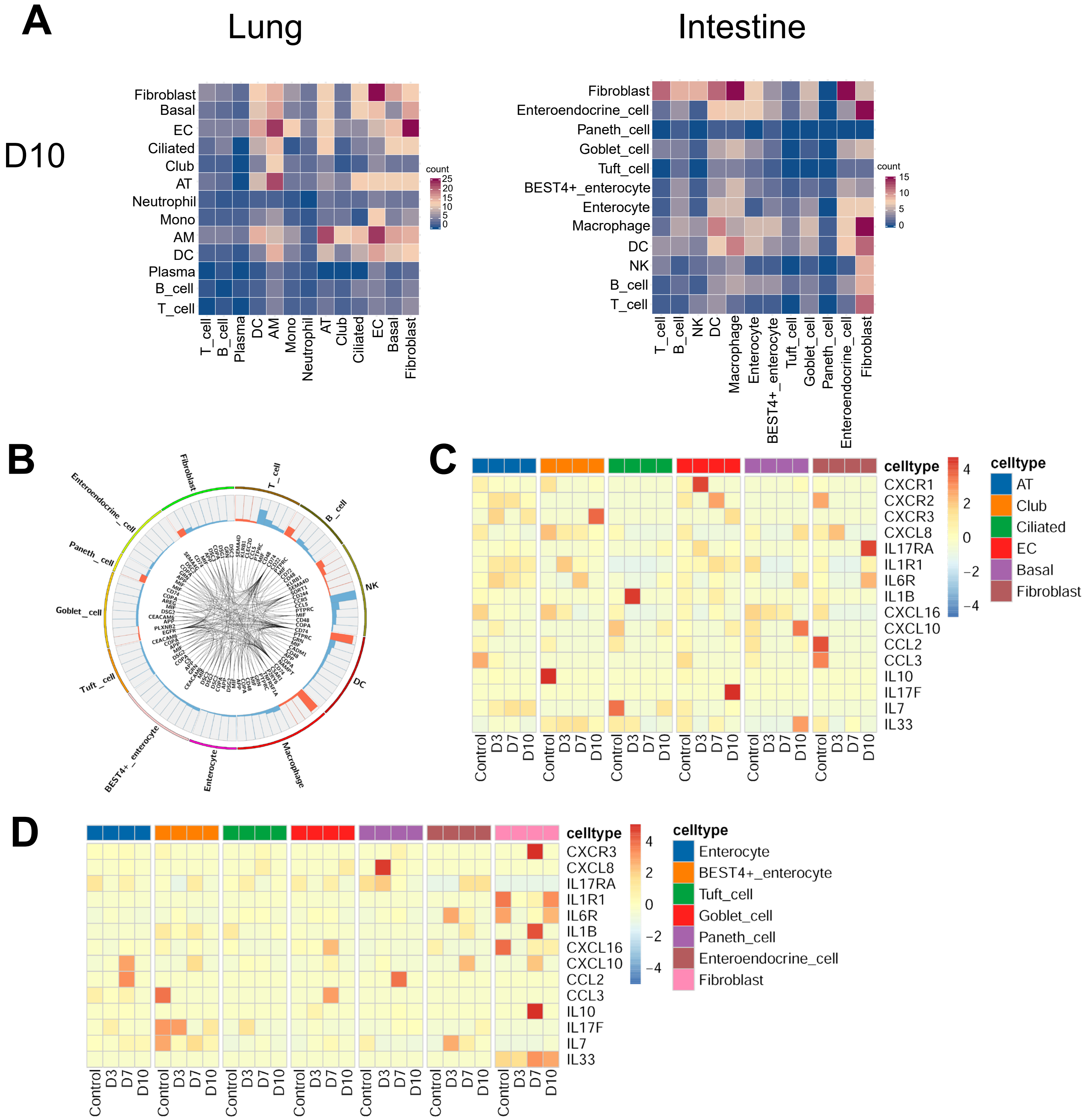

Figure S5: Expression of chemokines, cytokines and receptor–ligand pairs genes in infected-associated tissues, related to Figure 7. (A) Cell–cell communication was identified by cellphone DB at 10dpi vs. control sample for SARS-CoV-2–infected macaques in the lung and small intestinal tissue. The darker the color intensity is, the more pairs of receptor–ligand interactions there are between cells. (B) Analysis of receptor-ligand pairs across different cell clusters from the intestine of SARS-CoV-2–infected macaques at 3 dpi, 7 dpi and 10 dpi . All shown interactions were statistically significant based on a permutation test, and arrows denote directionality from ligand to receptor. The red bar represents the receptor, and the blue color bar represents the ligand. The height of the bar represents the average expression of the receptor or ligand gene. (C-D)Heatmap showing normalized average expression of the indicated chemokines and cytokines compared with normal controls with the scale function of pheatmap at 3, 7, and 10 dpi in tissue cells from the lung (C) and intestine (D).

Table S1: Clinical signs observed in rhesus macaques infected with SARS-CoV-2, related to Figure 1.

Animal	Clinical signs observed 1 to 3 dpi	Clinical signs observed 4 to 7 dpi	Clinical signs observed 8 to 10 dpi
Rh1	Normal appetite; Normal and alert; Moving without prompting;	N/A	N/A
	Euthanized 3 dpi		
Rh2	Normal appetite; Normal and alert; Moving without prompting;	Reduced appetite; Slow/quiet, hunched, but alert, interested; Moving without prompting;	N/A
		Euthanized 7 dpi	
Rh3	Normal appetite; Slow/ quiet, hunched, but alert, interested; Moving without prompting;	Reduced appetite; Slow/quiet, hunched, but alert, interested; Moving without prompting;	N/A
		Euthanized 7 dpi	
Rh4	Normal appetite; Slow/ quiet, hunched, but alert, interested; Moving without prompting;	Reduced appetite; Quieter, hunched, but alert, interested; Moving without prompting;	Reduced appetite; Slow/quiet, hunched, but alert, interested; Moving without prompting;
			Euthanized 10 dpi
Rh5	Normal appetite; Slow/ quiet, hunched, but alert, interested; Moving without prompting;	Reduced appetite; Quieter, hunched, but alert, interested; Moving without prompting;	Reduced appetite; Slow/quiet, hunched, but alert, interested; Moving without prompting;
			Euthanized 10 dpi

Animals were observed daily according to a standardized scoring sheet (Zheng et al., 2020a). N/A, not available.

Table S2: The canonical markers of different kinds of cells in lung and small intestine, related to STAR Methods

Intestinal tissue	
T_cell	CD3D, NKG7
B_cell	MS4A1, CD79B
DC	MNDA, CLEC9A
NK	GZMA, KLRB1
Macrophage	CD68, C1QC
Enterocyte	EPCAM, PIGR
BEST4+_enterocyte	BEST4
Tuft_cell	DCLK1, ALOX5
Paneth_cell	DEFA6
Enteroendocrine_cell	CHGA, CHGB
Fibroblast	DCN, COL1A1
CD8_Teff	CD8A, NKG7, GZMB, KLRD1
Tfh	MAF, CD200, ICOS, CXCR5
Naïve_T_or_Tcm	SELL, TCF7, LEF1, CCR7
Lung tissue	
T_cell	CD3D, NKG7
B_cell	MS4A1, CD79B
Plasma	JCHAIN, MZB1
DC	IRF8, CLEC9A
Alveolar_Macrophage	CD68, C1QC
Mono	CD14,VCAN
Neutrophil	CSF3R, CAMP
AT	SFTPB, SFTPC
Club	SCGB1A1, SCGB3A2
Ciliated	PIFO, SNTN
EC	CDH5, PECAM1
Basal	KRT5, KRT15
Fibroblast	COL1A1, LUM
Teff	NKG7, GZMB, KLRD1, CCL5
Naïve_T_or_Tcm	SELL, TCF7, LEF1, CCR7
Trm	MAF, ANXA2, CRIP1, CD69
cDC1	XCR1, CLEC9A
cDC2	CD1C, FCER1A
Mig_DC	LAMP3, CCR7
pDC	LILRA4, TCF4
Classical_mono	CD14, VCAN, SELL
Nonclassical_mono	FCGR3
Type_I_Pneumocytes	AGER, CAV1

Type_II_Pneumocytes	SFTPB, SFTPC, LAMP3